

# SEGMENTED AND SHIELDED STRUCTURES FOR REDUCTION OF THERMAL EXPANSION-INDUCED TILT ERRORS

A. John Hart (ajhart@mit.edu), Alexander H. Slocum  
*Precision Engineering Research Group  
Massachusetts Institute of Technology, Cambridge, MA*

## I. INTRODUCTION

Microscopes are now utilized for a wide variety of tasks in addition to imaging, requiring complex laser optics, metrology tools, and precision motion mechanisms in conjunction with the basic microscope structure. These technological advances have made single molecule detection and analysis possible, driving interest in measurements with sub-nanometer precision. However, structural designs of current microscopes, which have retained a similar cantilevered shape for decades, make such advanced setups cumbersome, difficult to reconfigure, and unacceptably sensitive to thermal and mechanical disturbances. Significant improvements in the flexibility, stability and resolution of the microscope are needed.

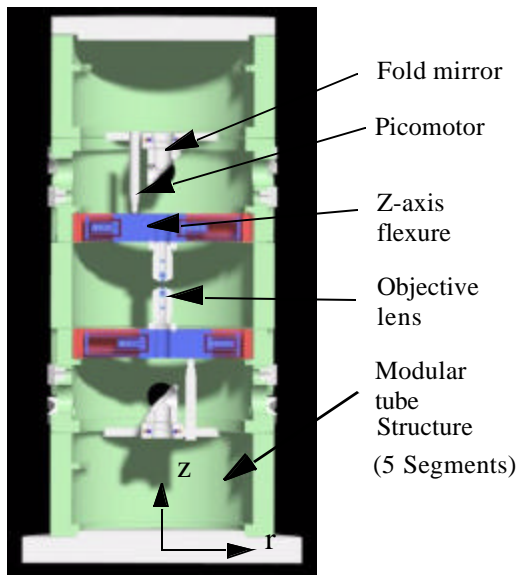


Figure 1: Segmented tube microscope structure.

The High Precision Microscope (HPM) project, headquartered at the University of Illinois Laboratory for Fluorescence Dynamics with the mechanical design and testing conducted by the MIT

Precision Engineering Research Group, is developing a novel microscope system for single molecule experiments. The main feature, shown in Figures 1 and 2, is a series of five aluminum rings connected by kinematic couplings. The sample stage and lens optics are fastened to the inside surfaces of the ring modules, and the optical signals are transmitted to and from the lasers and signal processing equipment (placed away from the structure) by fiberoptic cables. This paper focuses on the thermal error modeling and testing of the HPM structure.

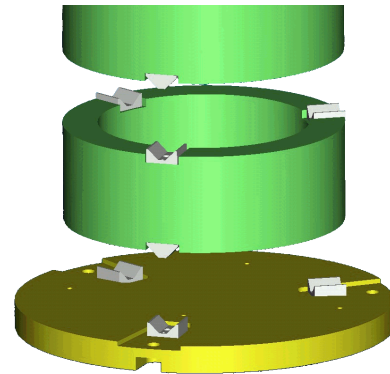


Figure 2: Tube interfaces using canoe ball kinematic couplings.

## II. STRUCTURE DESIGN

Compared to a traditional cantilevered microscope design or a single-tube structure, the segmented tube structure has two main performance advantages. First, as shown by the simulated isotherms in Figure 3, the gaps between the segments restrict heat flow parallel to the axis of the tube stack. As a result, the temperature distribution around the circumference of each tube under a thermal gradient in the ambient, characterized most simply by the difference in the surface temperature between opposite sides of the tube surface, is more uniform with a segmented design. Increasing the angular uniformity of the temperature distribution decreases the tilt error of the structure. Furthermore,

infinity corrective objectives used in microscopy are not sensitive to uniform axial expansion, and radial expansion is not an issue as long as the center point where the objectives reside remains in the same radial position as the elements along the optical path.

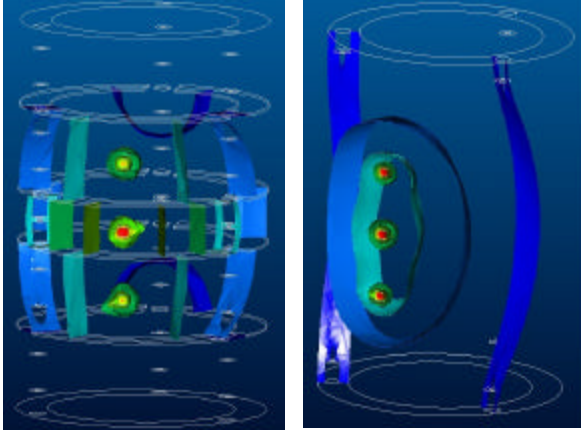


Figure 3: Steady-state isotherms on segmented and one-piece tube structures

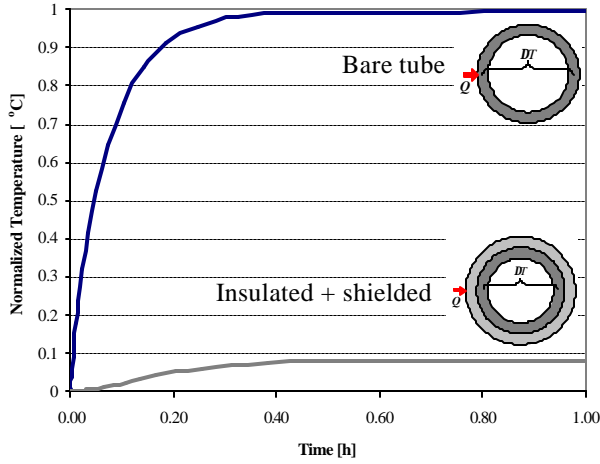


Figure 4: Simulated performance of shielded and insulated tubes under step heat input.

Each tube segment can be further thermally stabilized by insulating and shielding its outside surfaces. Here, the inner structural ring is covered by a layer of fiberglass insulation, and held in place by a thin shield having high thermal conductivity (e.g. aluminum or copper). The shield quickly dissipates temperature differences around its circumference [1], and the insulation increases the thermal resistance between the outside shield and the load transmission points on the inner ring. Figure 4 compares

the simulated performance of a bare tube cross section to that of an insulated and shielded tube cross section. For the dimensions chosen, the shielding and insulation more than doubles the response time to a step input, and the steady-state temperature difference across the shielded and insulated tube is one-tenth of that across the bare tube. Similar results are noted when an oscillating input is tested; the shielding and insulation both delay and significantly reduce the magnitude of the disturbance on the structural section.

Second, the HPM design benefits from precision mechanical alignment of the optical axes, enforced by the inherent repeatability of the precision-ground “canoe ball” (named as such because the large-radius spherical surfaces look like the bottom of a canoe) kinematic couplings between the segments. Several studies have demonstrated sub-micron repeatability of kinematic couplings [2,3,4,5], and the detailed analysis methods for considering effects such as nonrepeatability due to friction [6] and interchangeability errors due to manufacturing variation [7] are now well-known. The equal-angle groove arrangement of the kinematic coupling averages the radial thermal expansion errors of the tubes to minimize the drift of the central optical axis. Different optical modules can be attached to pre-calibrated “replacement” tube segments, and the segments can be interchanged to reconfigure the setup of the HPM without requiring coarse re-calibration of the instrument each time.

### III. APPROXIMATION OF THERMAL ERRORS

A difference in axial thermal expansion induced by a circumferential temperature gradient around the tube structure causes the tilt error motion shown in Figure 5. In terms of the temperature profiles along the heated ( $T_h$ ) and non-heated ( $T_n$ ) sides, the material coefficient of thermal expansion ( $\alpha_t$ ), and the initial height of the stack ( $L_o$ ), the differential expansion ( $\delta$ ) of the opposite sides of the stack is

$$\delta = \alpha_t L_o (\bar{T}_h - \bar{T}_n) = \alpha_t \left( \int_0^{L_o} (T_h(z) - T_n(z)) dz \right). \quad (1)$$

Hence, the tilt angle ( $q_{tilt}$ ) of the top plate is

$$\theta_{tilt} = \text{atan} \left( \frac{\alpha_t L_o (\bar{T}_h - \bar{T}_n)}{D_s} \right). \quad (2)$$

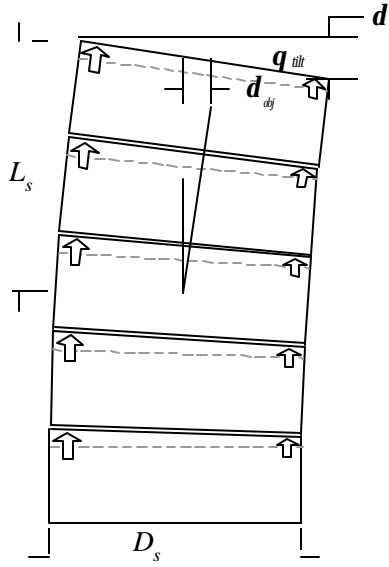


Figure 5: Tilt error motion of segmented structure.

The distance ( $d_{obj}$ ) by which the position of the sample moves with respect to the optical backplane (where the lasers are focused at the top of the structure) is

$$\delta_{obj} = L_s \frac{\alpha_t L_o (\bar{T}_h - \bar{T}_n)}{D_s}. \quad (3)$$

Treating the circumferential path of heat conduction around the structure as through a linear body with effective area  $A$ , effective length  $L$ , and material thermal conductivity  $k$ , the heat flow  $Q$  is

$$Q = \frac{(\bar{T}_h - \bar{T}_n)}{L} Ak. \quad (4)$$

Rearranging (3) and substituting into (2):

$$\delta_{obj} = L_s \frac{\alpha_t L_o L Q}{D_s Ak}. \quad (5)$$

Therefore, with the goal to minimize  $d_{obj}$  for a chosen structure geometry, the best material for steady-state performance is one with maximum thermal conductivity per unit of tendency to thermally expand,  $k/\alpha_t$ .

In terms of transient performance, the penetration depth  $x$  of temperature change through the structure at time  $t$  after a constant thermal disturbance is applied is

$$x = \frac{\sqrt{\alpha t}}{Fo}, \quad (6)$$

where  $Fo$  is the Fourier number based on the structure geometry [8], and  $a$  is the material thermal dif-

fusivity. Assuming fixed geometry, the best structure material for transient performance is one with maximum  $a/a_t$ .

## IV. EXPERIMENTS

### A. Setup and Procedure

The thermal stability of the microscope structure was evaluated by applying localized heat inputs to its outside surface, and measuring the resulting circumferential and axial temperature distributions around the tubes, as well as the tilt motion of a top reference plate. Two structures were tested: the five-segment aluminum structure shown in Figure 6, with 12" outside tube diameter, 1.5" wall thickness, 25" total height, and 250 mm radius stainless steel canoe ball couplings between the segments; and a structure with a single tube having equivalent dimensions to the stack of five segments. Later, each tube was covered with 1" of fiberglass insulation ( $k = 0.03$  W/m-K) and a 1/16" aluminum shield.

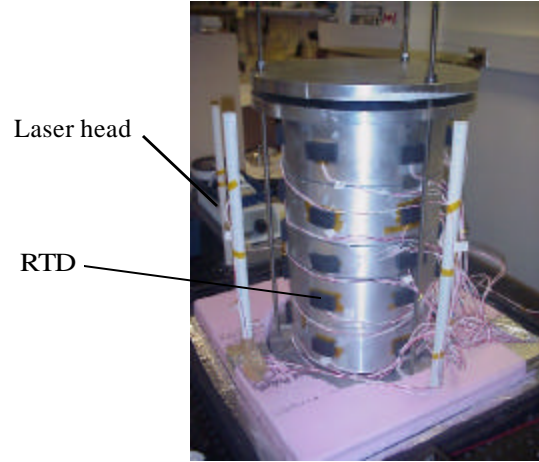


Figure 6: Prototype segmented structure, instrumented for thermal error measurements.

The temperature distribution on the structures and in the surrounding air was monitored using three-wire platinum RTD's (resistive temperature detectors). The RTD's were wired to a National Instruments LabView Data Acquisition System with 16-bit D/A conversion of the measured voltage giving resolution of 0.009 °C.

Angular drift was measured using a Zygo differential plane mirror interferometer (DPMI) [5], mounted to a 5" diameter aluminum column placed

within the stack assembly. The DPMI sensed the tilt of a reference mirror mounted to a horizontal reference plate attached to the top of the tube set. Temperature readings from the surface of the central column showed that it was sufficiently isolated from thermal gradients in the tube structure to be a reference mounting for the interferometer.

Thermal disturbances were applied to the structure using Minco copper thin film heating elements, each measuring 1/2" x 1/2". Three sources were mounted directly to the structure, one each at the vertical midpoints of the three center tubes, aligned vertically parallel to the single axis of the interferometer. The sources were wired in a parallel circuit.

The test apparatus (excluding the laser source) was placed in an insulated chamber constructed of 4" thick extruded polystyrene (Styrofoam), and mounted on an air-shock isolation table. Single-point readings from the interferometer and each RTD were taken once per minute, with a six-hour-long 3W (5V, 0.6A) step input starting one hour after data acquisition began. Real heat inputs to a microscope structure may be as small as 0.1 W from low heat-dissipation actuators, or as high as 30 W caused by an operator standing close to a bare structure [1].

In addition to the experimental setup, finite element models of the two structures were built in Pro/MECHANICA™. As a simplification, the kinematic coupling balls and grooves between the segments were replaced by sets of square (a very liberal estimate given the true nearly point contact) contacts between the tube-to-tube gaps. Derived from thermobuoyant convection relations for vertical cylinders and horizontal plates [9], a uniform steady-state loss coefficient was defined on each external surface of the model. The tilt angle of the structure was calculated using the results of the thermal analysis as a temperature boundary condition for a structural analysis.

### B. Results

Figure 7 compares the measured tilt error of the single-tube structure, the segmented structure, and the segmented structure with insulation and shielding on the three heated segments. At steady-state, the bare segmented structure drifts approximately 40% less than the one-piece structure (0.61 arcsec vs. 0.86 arcsec). Insulation and shielding reduce the

maximum drift to only 0.24 arcsec, a 75% overall improvement. The differences in the rates of drift are also significant; the drift of the segmented structure within the first hour of heating (a typical duration of an experiment with the HTM) is 60% less than of the single-tube design, due to the shorter time it takes for heat to reach the axial conduction constraints imposed by the gaps between the tube segments. This initial rapid drift is not seen with the shielded and insulated structure because the insulation delays penetration of the disturbance to the inner tube until well after the disturbance has propagated fully around the circumference of the shield.

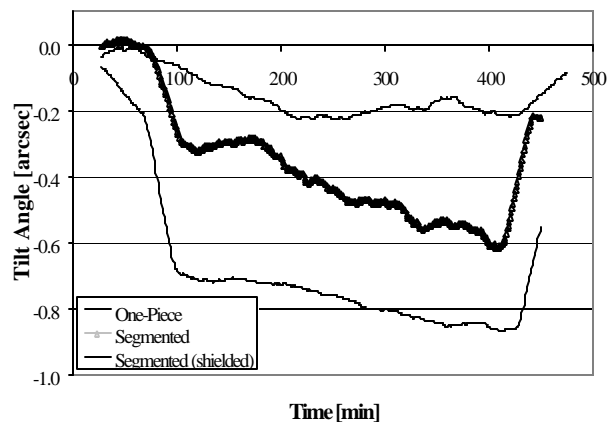


Figure 7: Measured tilt error (15-minute moving average of interferometer readings)

| Level | Seg<br>FEA | Seg<br>Meas. | OnePc<br>FEA | OnePc<br>Meas. |
|-------|------------|--------------|--------------|----------------|
| 1     | 0.01       | 0.00         | 0.07         | 0.06           |
| 2     | 0.12       | 0.13         | 0.12         | 0.09           |
| 3     | 0.18       | 0.21         | 0.12         | 0.12           |
| 4     | 0.12       | 0.12         | 0.12         | 0.09           |
| 5     | 0.01       | 0.00         | 0.07         | 0.06           |

Table 1: Simulated and measured circumferential temperature differences [°C] (level 1 = bottom).

Table 1 compares the measured steady-state temperature differences at the centerline level of each tube to those simulated by FEA. These differences are 0.03 °C or less at all levels of both structures, within reasonable tolerances for validation of the finite element model as a tool for design optimization. Discrepancies arise because the simulation is a steady-state calculation only, the coupling coupling

contacts are idealized, and the convection coefficient on the outer surface of the models is uniform. The FEA model predicts tilt of the segmented and one-piece designs of 0.50 and 0.75 arcsec, both approximately 15% less than the measured values taken after 450 minutes of testing.

## V. DESIGN STUDIES

Validation of the finite element models permitted their use for design optimization. First, a performance comparison between materials gave the tilt values listed in Table 2, showing copper to be the best traditional metal for the structure. Investigation of ceramics and other low-expansion materials (e.g. Invar) is also worthwhile.

| Material         | Tilt |
|------------------|------|
| Aluminum (6061)  | 1.00 |
| Copper           | 0.35 |
| Brass            | 1.40 |
| Stainless (1040) | 4.20 |

Table 2: Simulated tilt errors for common structural metals, normalized relative to value for Aluminum.

Next, keeping the total tube length and the inside diameter as packaging constraints, the tube thickness of both structures was varied within reasonable bounds of 1.0" and 2.5". Then, for the segmented structure, total length, inside diameter, and thickness were held constant and the number of segments was varied. For simplicity of the analysis, one 3W heat source was applied at the horizontal centerline of the structure.

Figure 8 shows that the error motion monotonically decreases with increasing tube thickness for the one-piece structure and for the structure with five segments. Hence, a better design is one with five thick segments, and a structure with five segments always outperforms a one-piece structure of the same thickness. The data series marked by triangles shows the error motion with thickness fixed at 1.5", with the number of segments varying (in increments of two) from one to nine. When the results with varying thickness and with varying number of segments are collapsed onto the same plot in terms of the segment height to thickness ratio, Figure 9 results. Here, the (square- and diamond-marked) curves for when thickness is varied are similar in

shape (within the convergence confidence of the simulation), and are simple translations along the triangle-marked curve for when the number of segments is varied. These results demonstrate that constraining the axial flow using a shorter segment is advantageous only until the effect of the decreased thermal capacitance of the segment takes over, after which the greater overall heating of the segment increases the magnitude of the thermal expansion.

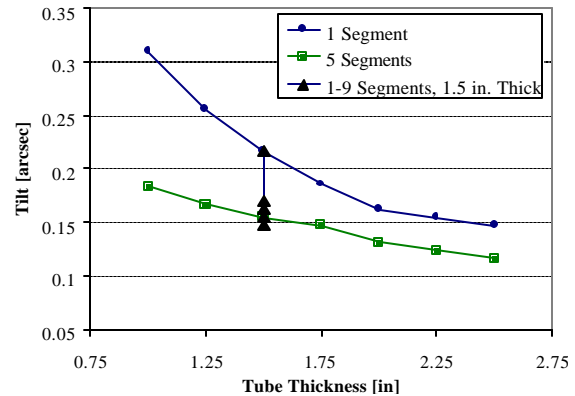


Figure 8: Angular deflection of copper structures with varying tube thickness

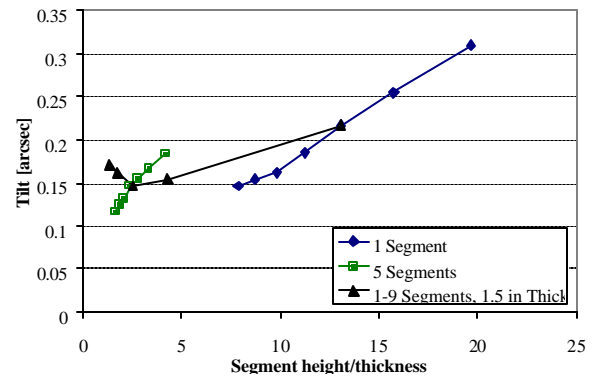


Figure 9: Angular deflection versus ratio of segment height to segment thickness

| Design   | Drift [nm] |
|--|------------|
| One-segment Al (measured)                                | 533        |
| Five-segment Al (measured)                               | 376        |
| Five-segment Cu (FEA)                                    | 133        |
| Five-segment 2.5" thick Cu (FEA)                         | 99         |
| Five-segment 2.5" thick Cu, 2" insulation. 1/16" shield. | 26         |

Table 3: Predicted linear drift of several designs.

Finally, Table 3 compares the performance of various designs considered throughout the study, in terms of the translational error at the optical backplane, computed according to Eq. 3. Simulation predicts that a five-segment copper structure, with 2.5" thick segments covered by 2" of insulation and 1/16" copper shielding will drift nm over several hours, a 20-fold improvement over the initial aluminum segmented structure design

## VI. CONCLUSIONS

The results of the thermal study of the HPM structure demonstrate the feasibility of a segmented design for modular serial assemblies, such as instrumentation structures including microscopes and high-precision reconfigurable industrial equipment such as large coordinate measuring machines or assembly robots. The design significantly reduces the thermal sensitivity of a tubular structure, while maintaining structural integrity and offering the flexibility of disassembly, reconfiguration, and reassembly using kinematic couplings. Insulation and shielding is shown to significantly reduce steady state thermal errors. Experimental results validate use of sequential thermal and structural finite element simulations for design optimization of segmented structures based on steady-state drift approximations. Measurement and modeling of the performance of the structure designs under fluctuating heat inputs will be performed next, after which a new structure will be built and tested in operation as a high-precision microscope.

## ACKNOWLEDGEMENTS

John Hart gratefully acknowledges the support of a National Science Foundation Graduate Research Fellowship and a Fannie and John Hertz Foundation Fellowship. Philip Loiselle and Way Luu helped machine, assemble, wire, and test the prototype structures. Way's work was supported by the Ralph L. Evans (1948) Endowment Fund for undergraduate research (UROP) at MIT. Jason Sutin of the University of Illinois Laboratory for Fluorescence Dynamics guided the design requirements for the HPM structure.

## REFERENCES

- [1] Ruiji, Theo. "Ultraprecision Coordinate Measuring Machine", Ph.D. Thesis, Eindhoven, The Netherlands, 2001.
- [2] Slocum, A. H. and A. Donmez. "Kinematic Couplings for Precision Fixturing - Part 2: Experimental Determination of Repeatability and Stiffness", *Precision Engg*, vol. 10, No. 3, July 1988.
- [3] Mullenheld, B. "Application of kinematic couplings to a grinding wheel interface", S.M. Thesis, University of Aachen (Germany), 1999.
- [4] Poovey, T., et al. "A Kinetically-Coupled Magnetic Bearing Test Fixture," *Precision Engg*, Vol. 16, No. 2, April 1994.
- [5] Slocum, A.H. Precision Machine Design, Society of Manufacturing Engineers, 1992.
- [6] Hale, L. and Slocum, A.H. "Optimal Design Techniques for Kinematic Couplings", *Precision Engg*, 2000, 25(2), 114-127.
- [7] Hart, A. J. "Design and Analysis of Kinematic Couplings for Modular Machine and Instrumentation Structures", S.M. Thesis, Massachusetts Institute of Technology, 2001.
- [8] Leinhard, J.H. IV, and J.H. Leinhard V. A Heat Transfer Textbook, Phlogiston Press, 2001.
- [9] Kaviany, M. Principles of Heat Transfer, Course Reader for Mechanical Engineering 370, University of Michigan at Ann Arbor, 1999.